

Article

Redefining Benggang Management: A Novel Integration of Soil Erosion and Disaster Risk Assessments

Xiqin Yan ¹, Shoubao Geng ¹ , Hao Jiang ¹ , Zhongyu Sun ¹, Nan Wang ², Shijie Zhang ³, Long Yang ¹ and Meili Wen ^{1,*}

¹ Guangdong Provincial Key Laboratory of Remote Sensing and Geographical Information System, Guangdong Open Laboratory of Geospatial Information Technology and Application, Guangzhou Institute of Geography, Guangdong Academy of Sciences, Guangzhou 510070, China; yanxiqin@gdas.ac.cn (X.Y.); gengshoubao@gdas.ac.cn (S.G.); jianghao@gdas.ac.cn (H.J.); sunzhyu@gdas.ac.cn (Z.S.); yanglong@gdas.ac.cn (L.Y.)

² National-Regional Joint Engineering Research Center for Soil Pollution Control and Remediation in South China, Guangdong Key Laboratory of Integrated Agro-Environmental Pollution Control and Management, Institute of Eco-Environmental and Soil Sciences, Guangdong Academy of Sciences, Guangzhou 510650, China; wnan@soil.gd.cn

³ Anhui and Huaihe River Institute of Hydraulic Research, Hefei 230088, China; shijie8433@163.com

* Correspondence: wenml@gdas.ac.cn

Abstract: In the granite regions of southern China, benggang poses a substantial threat to the ecological environment due to significant soil erosion. This phenomenon also imposes constraints on economic development, necessitating substantial investments in restoration efforts in recent decades. Despite these efforts, there remains a notable gap in comprehensive risk assessment that integrates both the erosion risk and disaster risk associated with benggang. This study focuses on a representative benggang area in Wuhua County, Guangdong province, employing transformer methods and high-resolution imagery to map the spatial pattern of the benggang. The integrated risk of benggang was assessed by combining soil-erosion risk and disaster risk, and cultivated land, residential land, and water bodies were identified as key disaster-affected entities. The machine-learning Segformer model demonstrated high precision, achieving an Intersection over Union (IoU) of 93.17% and an accuracy (Acc) of 96.73%. While the number of large benggang is relatively small, it constitutes the largest area proportion (65.10%); the number of small benggang is more significant (62.40%) despite a smaller area proportion. Prioritization for benggang management is categorized into high, medium, and low priority, accounting for 17.98%, 48.34%, and 33.69%, respectively. These priorities cover areas of 30.27%, 42.40%, and 27.33%, respectively. The findings of this study, which offer benggang management priorities, align with the nature-based solutions approach. Emphasizing the importance of considering costs and benefits comprehensively when formulating treatment plans, this approach contributes to sustainable solutions for addressing the challenges posed by benggang.



Citation: Yan, X.; Geng, S.; Jiang, H.; Sun, Z.; Wang, N.; Zhang, S.; Yang, L.; Wen, M. Redefining Benggang Management: A Novel Integration of Soil Erosion and Disaster Risk Assessments. *Land* **2024**, *13*, 613. <https://doi.org/10.3390/land13050613>

Academic Editor: Wojciech Zglobicki

Received: 21 March 2024

Revised: 29 April 2024

Accepted: 30 April 2024

Published: 2 May 2024



Copyright: © 2024 by the authors. Licensee MDPI, Basel, Switzerland. This article is an open access article distributed under the terms and conditions of the Creative Commons Attribution (CC BY) license (<https://creativecommons.org/licenses/by/4.0/>).

1. Introduction

Soil erosion stands as a formidable challenge in the contemporary environment [1], given its persistent ramifications on both ecosystems and social services [2]. The imperative for soil-erosion risk assessment is underscored by its pivotal role in informing the development of robust policies and interventions for water and soil conservation [3]. Several models have been instrumental in generating soil-erosion risk assessment maps [4], facilitating decision-making processes by pinpointing high-priority areas and delineating targeted measures for optimal efficacy [5]. For instance, Hu et al. [6] integrated remote-sensing information (RS), geographic information system spatial analysis technology (GIS), and a soil-erosion risk assessment model to estimate the soil-erosion risk of the Yanshan Reservoir catchment. Bamutaze et al. [7] investigated the intersection between empirically derived and farmers' perceived soil-erosion risk in a medium-sized catchment on

the Ugandan side of mountain Elgon. However, a conspicuous gap persists in the literature, where a substantial proportion of studies overlook a distinctive soil-erosion type in southern China—namely, the dominant fragmented erosional landform often referred to as “Benggang” [8,9]. According to existing publications, “Benggang”, “Collapsing hill” and “Collapsing gully” have been most widely used in Chinese journals, while “Collapsing gully”, “Gully” and “Benggang” are dominantly used in international scientific reports [9].

The term “benggang” originates from the Meizhou area in Guangdong Province. The “beng” in benggang refers to an erosion process primarily characterized by collapse, while “gang” denotes the original geomorphological form where this type of erosion frequently occurs. This description aptly captures both the erosive process and the geomorphological features of benggang. This erosion phenomenon has garnered national attention in China due to its profound impacts on ecosystems and social services, particularly within tropical and subtropical regions [9]. This conspicuous absence emphasizes the critical need to tackle the distinct challenges associated with benggang, situating them within the expansive scope of soil-erosion studies and risk analysis.

Benggang, characterized as a specific form of soil erosion within the red soil region [10], predominantly emerges in the humid monsoon climate areas of the tropical and subtropical zones in southern and southeastern China [11]. Notably, benggang exhibits a substantial erosion modulus, posing a significant threat to the ecological environment and imposing constraints on economic development. Survey data from seven provinces in southern China in 2009 estimated approximately 239.1 thousand instances of benggang [12]. The consequences of benggang are profound, leading to the loss of topsoil and rendering cultivated land unusable [13]. Over the period from 1949 to 2005, a staggering 380,000 hectares of cultivated land were either destroyed, buried, or abandoned due to benggang activities, resulting in a direct economic loss of 550 million yuan [13]. Additionally, the sediment generated by benggang is transported downstream, contributing to the silting of channels, ponds, riverbeds, and reservoirs [12]. This downstream movement not only jeopardizes the safety of lives and property but also inflicts significant harm on agricultural production, the ecological environment, and the general well-being of people [14].

Benggang erosion has received abundant attention in the past few decades [15]. With an increase in research and achievements from 2010 to the present, research efforts have concentrated on various aspects of benggang, including classification [16], development process [17], formation mechanism [18], and treatment measures [19,20]. These studies have provided theoretical guidance and a scientific basis [19,21] for the prevention and management of benggang [22]. However, many assessments regarding benggang risk primarily focus on potential risk. For instance, Wu [23] establishes four benggang susceptibility models using various methods and 12 benggang-related factors. Wei et al. [24] investigate the spatial susceptibility of benggang in Fujian province using three data-driven methods (multinomial logistic regression, random forest, and multilayer perceptron). Sun et al. [10], based on risk assessment theory, utilize information acquisition analysis and logistic regression to explore the feasibility of benggang risk assessment in Guangdong province. These methods are in line with those employed in landslide hazard studies [25,26].

However, there is a limited number of studies that have evaluated the priority of benggang management considering both soil-erosion risk and disaster risk. Most existing research focuses on potential risk prediction. The assessment of actual occurrence risk, as well as the urgency for management, has been somewhat overlooked. This gap is crucial as prioritizing benggang management is a key aspect of effective intervention strategies. Another challenge faced is the availability of reliable data on the number and location of benggang. The existing comprehensive and extensive data have been obtained from the Yangtze River Water Resources Commission of the Ministry of Water Resources. They conducted a comprehensive survey of benggang larger than 60 m^2 from August 2004 to November 2005 [27]. However, due to concerns about the accuracy and timeliness of this data, some studies have explored UAV-based (unmanned aerial vehicle) recognition of benggang. Shen et al. [28] used a semantic fusion of high-resolution digital orthophoto map

and digital surface model data from UAVs to recognize benggang, while Zhou et al. [29] monitored changes in benggang based on oblique aerial images from UAVs. Despite these efforts, identifying benggang at a regional scale remains challenging.

The benggang is prevalent in the red soil regions of southern China, specifically in seven provinces: Guangdong, Guangxi, Hunan, Jiangxi, Hubei, Anhui, and Fujian [30]. Within this context, Guangdong Province emerges as the most profoundly impacted area, hosting 107,800 benggang, which account for 45.1% of the total benggang occurrences in the southern region [10]. Huacheng Town in Wuhua County, Meizhou City, Guangdong Province, was chosen as the sample area due to its typical and representative nature in terms of benggang occurrence [31]. In this study, we introduce a novel approach by applying transformer models in machine learning to detect benggang. It further integrates assessments of erosion and disaster risks associated with existing benggang instances to provide a holistic risk evaluation. This innovative methodology aids in developing targeted management strategies. Moving beyond traditional sensitivity analyses of benggang incidents, this study offers more practical insights into the effective prevention and management of benggang. Our approach involves (1) utilizing remote-sensing images, deep machine learning, UAV technology, and field surveys to create a dataset of benggang spatial distribution of Huacheng Town, and (2) presenting a prioritization map for the management of benggang, considering perspectives of soil-erosion risk and disaster risk. The comprehensive risk assessment offers a scientific foundation for centralized and phased management of benggang.

2. Study Area and Methods

2.1. Study Area

The study was conducted in Huacheng Town ($23^{\circ}23' - 24^{\circ}12''$ N, $115^{\circ}18' - 116^{\circ}02'$ E) within Wuhua County, Guangdong province, situated in southern China (Figure 1). Wuhua County experiences a humid subtropical climate [32], characterized by an average annual temperature of 20°C . The region is endowed with ample rainfall, boasting an average yearly precipitation of 1515 mm [33]. Notably, the rainy season spans from April to September, constituting 76% of the total annual precipitation [13].

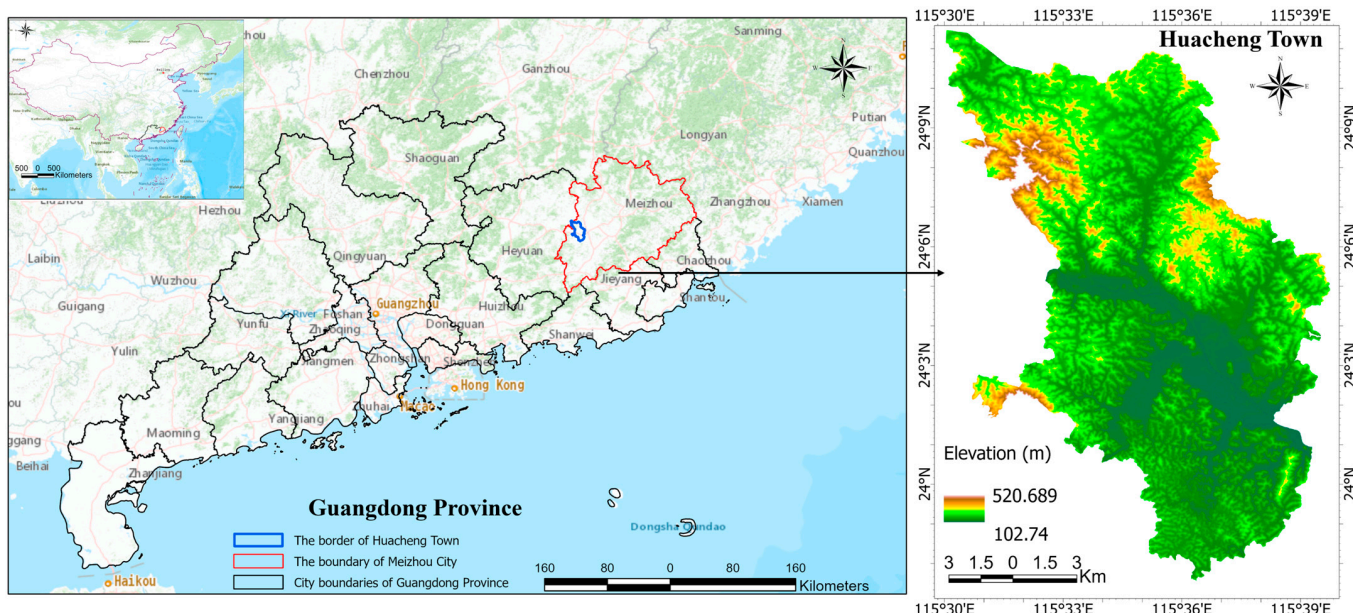


Figure 1. Location map of the study area.

Huacheng Town holds strategic significance as it is positioned upstream of the Mei-jiang River. Given its vulnerability to benggang occurrences, this area has the potential

to inflict substantial ecological harm downstream. Consequently, the study designates Huacheng Town as a representative region to evaluate and prioritize the management measures for benggang to mitigate potential ecological threats in the middle and lower reaches of the Meijiang River.

2.2. Data Sources and Methods

2.2.1. Data Sources

The dataset utilized in this study comprises essential geospatial information, encompassing a Digital Elevation Model (DEM), land use data, vector boundaries delineating the research area, and high-precision Google imagery. Table 1 provides an overview of the key components of this comprehensive dataset.

Table 1. Data sources and formats.

Data types	Time	Spatial Resolution	Format	Data Sources
DEM	2020	12.5 m	Raster	https://nasadaacs.eos.nasa.gov/ , accessed on 8 April 2020
Land use	2020	30 m	Raster	https://www.resdc.cn/DOI/DOI.aspx?DOIID=54 , accessed on 20 May 2020
Vector boundary	2020	—	Polygon	https://www.resdc.cn/DOI/DOI.aspx?DOIid=121 , accessed on 20 May 2020
Benggang	2022	0.6 m	Raster/Polygon	https://mt1.google.com , accessed on 30 June 2022
GF1	2021	2 m	Raster	http://gdgf.gd.gov.cn/GDGF_Portal/index.jsp , accessed on 18 December 2021

2.2.2. Risk Assessment of Benggang

Benggang refers to the erosion phenomenon where the weathered mantle of slope soil or rock separates, collapses, and accumulates under the combined effects of gravity and hydraulic forces. The management of benggang requires a systematic approach, encompassing a comprehensive understanding of their distribution and severity. Management measures involve detailed analysis, evaluation, and implementation at the watershed scale. This includes establishing a priority sequence for managing individual benggang, formulating differentiated prevention and management strategies based on varying hazard levels, and coordinating ecological restoration efforts upstream and downstream within the watershed. The study's analysis encompasses the following components (Figure 2).

(I) Benggang identification

The identification of benggang was achieved through a sophisticated machine-learning approach employing remote-sensing images. The detailed methodology is outlined below.

(1) Data acquisition: Google satellite images of Huacheng Town spanning the years 2020 to 2022 were downloaded from the link (<https://mt1.google.com>, accessed on 30 June 2022). The selected zoom level was set to 18, providing a spatial resolution of approximately 0.6 m.

(2) Training sample collection: Initial training samples of benggang were acquired through a combination of visual interpretation of Google Earth and GF-1 images.

(3) Machine learning: The Segformer model was employed for machine learning [34]. This model is specifically designed for tasks like image segmentation, making it well-suited for the identification of benggang. Suspected benggang were meticulously identified during this phase.

(4) Dataset verification and refinement: The machine-learning dataset of benggang was rigorously checked and verified through field surveys and UAV images. In the step, 13 control points were investigated and three types (benggang, bare land, and quarry) were verified. This multi-layered verification process ensured the accuracy and reliability of the dataset. Further refinement of the machine-learning dataset was conducted through meticulous checking and corrections, enhancing the overall quality and precision of the benggang identification.

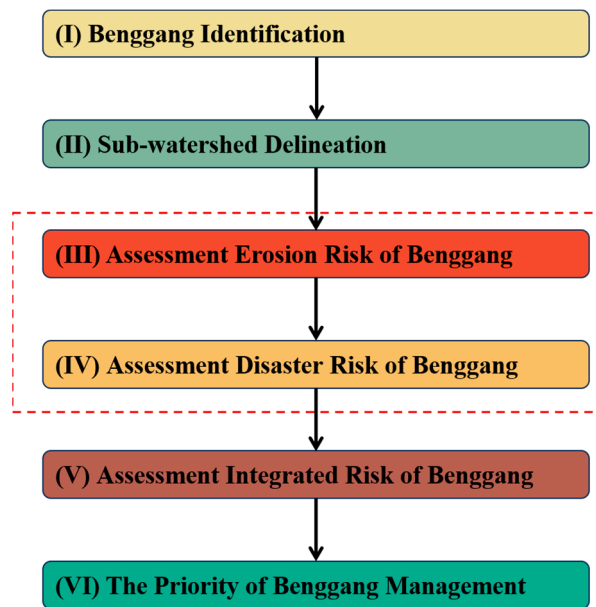


Figure 2. Comprehensive risk assessment framework for benggang. The combination of erosion risk (III) and disaster risk of benggang (IV) in the red dashed rectangle can be obtained (V) integrated risk of benggang.

(5) Accuracy Assessment: The accuracy of the benggang extraction results was assessed using established metrics, including accuracy (Acc), average accuracy ($mAcc$), Intersection over Union (IoU), and mean Intersection over Union ($mIoU$) [35]. These metrics are commonly employed in the evaluation of machine-learning models, particularly for image-segmentation tasks, providing a comprehensive assessment of the model's performance [36].

$$Acc = \frac{TP + TN}{TP + TN + FP + FN}$$

where Acc is the Accuracy, TP is the number of true positives (correctly predicted positive samples), TN is the number of true negatives (correctly predicted negative samples), FP is the number of false positives (incorrectly predicted positive samples), FN is the number of false negatives (incorrectly predicted negative samples).

$$mAcc = \frac{1}{N} \sum_{i=1}^N Acc_i$$

where $mAcc$ is the average accuracy, and N is the number of classes or categories.

$$IoU = \frac{TP}{TP + FP + FN}$$

where IoU is the Intersection over Union, TP is the number of true positives (as defined above), FP is the number of false positives (as defined above), and FN is the number of false negatives (as defined above).

$$mIoU = \frac{1}{N} \sum_{i=1}^N IoU_i$$

$mIoU$ is the Mean Intersection over Union, and N is the number of classes or categories.

(II) Sub-watershed delineation

The delineation of sub-watersheds is a crucial step in hydrological analysis, and the methodology employed in this study is outlined as follows. Firstly, a DEM with a spatial

resolution of 12.5 m serves as the foundational dataset. Secondly, utilizing the hydrological analysis module provided by ArcGIS, a series of essential processes including filling, flow direction, and flow accumulation is undertaken to derive the hydrological characteristics of the landscape.

The sub-watershed delineation ensures a systematic and comprehensive subdivision of the study area into distinct hydrological units. Each sub-watershed represents a discrete drainage area contributing to a particular point or outlet within the larger study area.

(III) Assessment of erosion risk of benggang

Assessment of erosion risk of benggang begins with the fundamental assumption that larger benggang areas are indicative of increased hazards. This assumption is grounded in the idea that larger benggang may pose greater risks to the landscape. The density analysis tool, available in ArcGIS, is a central component of the methodology. This tool facilitates the calculation of density based on specified computation units (sub-watershed) and associated weights (benggang area).

Sub-watersheds are selected as the computation units for the density analysis that enable a localized examination of erosion risk within distinct hydrological units. The benggang area is designated as the weight for the density analysis, which means that the area covered by benggang serves as a significant factor in the calculation of benggang density. Larger benggang areas are given more weight in the analysis.

The computed normalized benggang density values form the erosion-risk index for the study area. This index provides a standardized measure of erosion risk associated specifically with benggang within each sub-watershed, which offers valuable insights into the localized dynamics of benggang, aiding in the formulation of targeted and effective erosion management strategies for vulnerable areas within the study region.

(IV) Assessment of disaster risk of benggang

The assessment of disaster risk associated with benggang considers causative factors, disaster-prone environments, and the vulnerability of affected entities. We acknowledged that the magnitude of natural disasters is determined by causative factors and the disaster-prone environment. Causative factors, often rare or extreme events in the natural or human environment, lead to adverse effects on human life, property, and various activities, resulting in disaster scenarios.

Based on land use types and socio-economic development characteristics of the study area, the primary entities prone to disasters during benggang events are identified. These entities include cultivated land, residential land, and water bodies.

Since benggang and landslide hazards share similarities, insights from landslide-related research are applied for risk analysis. The proximity of an entity to the benggang source is considered a crucial factor influencing disaster risk. A buffer-zone method is employed to assess the potential impact of benggang. Distances from the benggang source are categorized into different ranges. These ranges are assigned normalized disaster risk values between 0 and 1. Results from previous studies indicate that benggang concentration is within specific distances [27]. Distances greater than 400 m from the benggang source are assigned a value of 0, indicating a low risk. Distances from 200 m to 400 m are assigned a value of 0.25, distances from 100 m to 200 m are assigned a value of 0.50, distances from 50 m to 100 m are assigned a value of 0.75, and entities within 50 m are assigned the highest risk value of 1.00.

By applying the assigned disaster-risk values to cultivated land, residential land, and water bodies, a disaster-risk map is generated. This map provides a visual representation of the potential risk associated with benggang for these specific entities within the study area. This methodology ensures a systematic and quantitative assessment of disaster risk, incorporating insights from landslide research and accounting for the proximity of entities to benggang sources.

(V) Assessment of integrated risk of benggang

The urgency of management becomes more pronounced when benggang occurs in areas with potential hazards. Therefore, the combination of both assessments allows for a more comprehensive evaluation of the integrated risk of benggang. The calculation formula is as follows:

$$P = P_f + P_w$$

where P represents the integrated risk of a specific benggang grid, P_f stands for the erosion risk of benggang, and P_w represents the hazard risk, which can be computed for a single disaster-affected entity (cultivated land, residential land, or water bodies), and can also be calculated for the overall risk considering multiple disaster-affected entities.

Benggang may pose hazards to various land uses, necessitating separate calculations for the integrated risk associated with different land uses. To facilitate a detailed integrated risk of benggang, a natural breakpoint method is applied to categorize integrated risk values into high-, medium-, and low-risk levels. This classification allows for a nuanced understanding of the potential risks and consequences associated with benggang across diverse land uses.

(VI) Identifying the priority of benggang management

Given the multitude of benggang occurrences in Huacheng Town, addressing all of them in the short term is impractical. Therefore, a prioritization analysis for benggang management becomes imperative, based on the integrated risk associated with each benggang.

If the comprehensive risks of cultivated land, residential land, and water bodies are considered collectively, equal weight is assigned to the integrated risks of these three types. The integrated risk of each benggang is extracted using “extract value to point” in ArcGIS as an indicator of the priority of benggang management. The higher the risk value, the higher the priority. The priority of management is then determined based on the high, medium, and low risks identified according to integrated risks. This approach ensures a systematic and efficient allocation of resources, with a focus on addressing the most critical benggang characterized by higher comprehensive erosion risk. By considering the specific risks associated with different land uses, the prioritization strategy allows for a targeted and strategic approach to benggang management efforts in Huacheng Town.

3. Results

3.1. Accuracy Evaluation of Benggang Identification

In our study, we employed advanced machine-learning algorithms for the recognition of benggang, utilizing high-resolution remote-sensing data. The results demonstrated promising accuracy in benggang identification, particularly with the Segformer model, showcasing a high degree of precision (Table 2). IoU and Acc recorded impressive values of 93.17 and 96.73%, respectively. To further substantiate the reliability of the machine-learning models, a thorough validation process was conducted using ground-truth data (Figure 3). The locations of the benggang, as depicted in Figure 3, were verified using GF_1 (2021) imagery and cross-checked through UAV images, coupled with on-site visits.

Table 2. Evaluation of single-class and average extraction results.

	Class	Acc (%)	IoU (%)
Single class	Benggang	93.17	96.73
	Background	99.89	99.94
Average	—	mAcc (%) 96.53	mIoU (%) 98.34

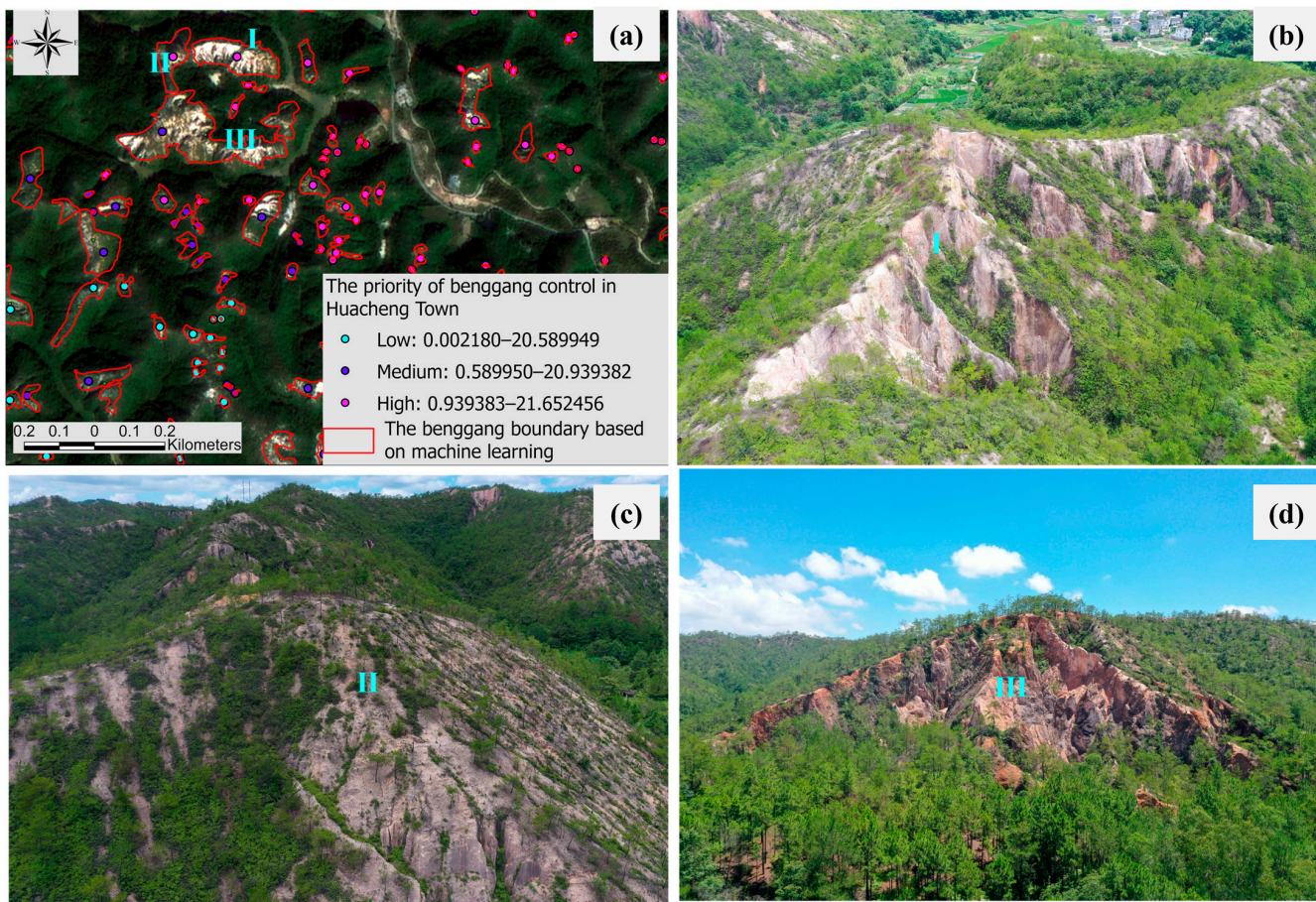


Figure 3. The verification of GF_1 image and UAV survey of benggang. (a) is the bottom map of the GF_1 image; the red polygon is the benggang range recognized based on machine learning, and the blue Roman numerals are the 3 benggang points for UVA (unmanned aerial vehicle) field verification; (b–d) are the images of benggang taken by UAV.

These findings underscore the potential of the Segformer model in significantly enhancing the precision and efficiency of benggang identification. The model's reliability offers valuable insights for benggang risk assessment and facilitates the development of effective mitigation strategies.

3.2. Benggang Distribution

Figure 4a shows the spatial distribution of benggang, a total of 2505 benggang in Huacheng Town, and their classification is based on size into small, medium, and large categories, with areas ranging as follows: 0 to 1000 m^2 , 1000 to 3000 m^2 , and $>3000\text{ m}^2$, respectively. Small benggang comprises 62.40% of the total, with an area proportion of 10.14%. Medium benggang comprises 22.69% of the total, covering an area proportion of 24.76%. Large benggang comprises 14.91% of the total, dominating with an area proportion of 65.10% (Figure 5). This distribution provides insights into the prevalence and spatial dominance of benggang across different size categories in Huacheng Town.

There is a correlation between benggang development and geomorphic characteristics [27], so we analyze the relationship between geomorphic characteristics and benggang area, aiming to provide the basis for management from the development characteristics of benggang. The majority of benggang occurrences are predominantly found in regions with elevations ranging from 125 to 325 m. Beyond an elevation threshold of 350 m, the frequency of benggang significantly diminishes, as illustrated in Figure 6a. The spatial distribution of benggang extends across a slope range from 0 to 40° . Notably, the normalized

integral value of the benggang area exhibits a pronounced peak at approximately 20° , as depicted in Figure 6b. Liao et al. [27] also discovered that the development of the landform value (HI) could serve as a predictive indicator of the erosion status of benggang. However, it is observed that HI has a stronger correlation with the occurrence of benggang than with lithology and rainfall patterns. Figure 6c demonstrates a trend where the area of benggang initially increases with HI, reaching a peak, and subsequently decreases, with the apex of benggang area corresponding to an HI index of about 0.5.

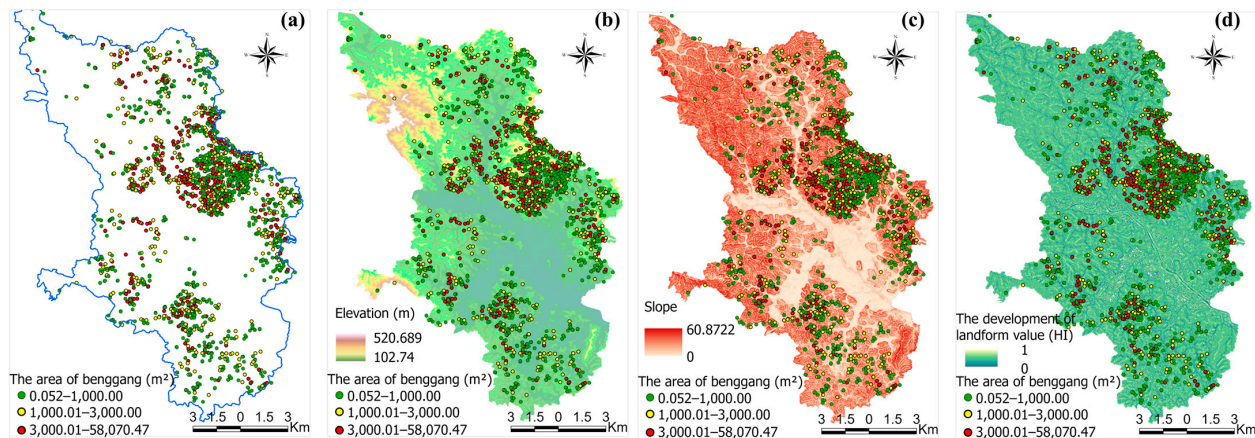


Figure 4. The spatial distribution of benggang types and topographic characteristics in Huacheng Town. (a) is the area of benggang, and (b–d) are the superposition diagrams of the area of benggang and the elevation, slope, and development of landform value, respectively, of Huacheng Town.m².

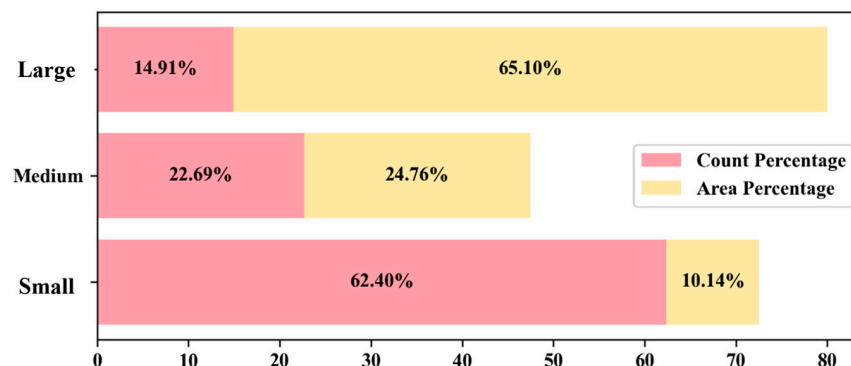


Figure 5. Area and quantity ratio of three categories of benggang.

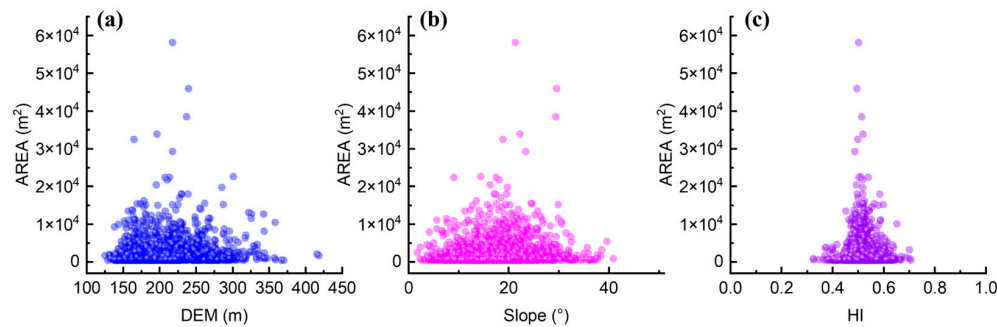


Figure 6. Relationship between benggang area and topographic characteristics. (a) is the relationship between the benggang area and elevation, (b) is the slope, and (c) is the HI (development of landform value).

3.3. Integrated Risk of Benggang

The density distribution of benggang exhibits a discernible pattern, characterized by higher density in the central region and lower density in the northern and southern areas

(Figure 7a). This spatial representation imparts valuable insights into the heterogeneous nature of erosion across Huacheng Town. The area density of benggang in Huacheng town exhibits a positively skewed distribution, predominantly characterized by smaller area densities (Figure 7b). Consequently, this information enables the development of a targeted and tailored approach to erosion management. By addressing the severity and distribution of benggang in specific regions, authorities and stakeholders can implement effective erosion management strategies with a focus on areas exhibiting higher risk and density.

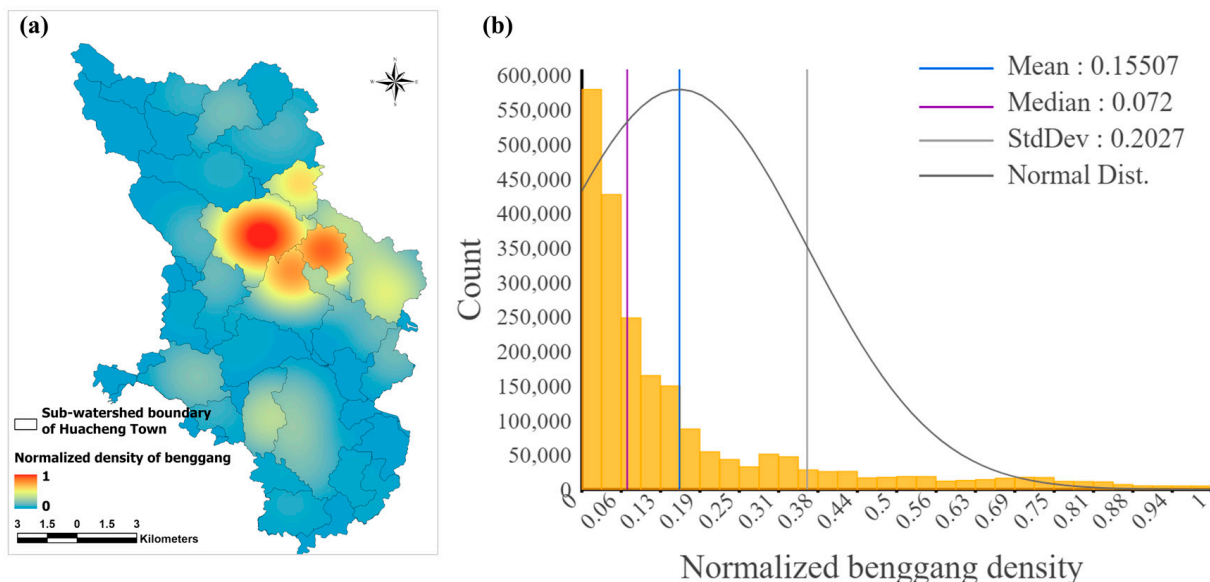


Figure 7. Spatial distribution and histogram of the normalized value of benggang density in Huacheng Town. (a) is the spatial distribution of the normalized benggang density index, and (b) is the histogram of the normalized benggang density index.

Remarkably, a relatively larger proportion of high disaster risk areas exhibit three land-use types (>50%) (Figure 8a–c). This critical information sheds light on the varying vulnerability of distinct land-use types to disasters induced by benggang. It serves as a foundation for the development of targeted risk-mitigation strategies tailored to the specific characteristics and susceptibilities of each land-use type. By overlaying the disaster risks of cultivated land, residential land, and water bodies, the integrated disaster risk for Huacheng Town is obtained (Figure 8d). The low-risk level area constitutes only 11.93% of the total, emphasizing the imperative need for comprehensive disaster management strategies. This is crucial to address the intricate risks associated with benggang in different land-use types.

By combining the erosion risk with the disaster risks for cultivated land, residential land, and water bodies, separate maps for the integrated risk of benggang for each land-use type are obtained (Figure 9a–c). Notably, regions with high risk for cultivated land cover a substantial proportion, accounting for 28.76%. Areas with high risk for all three land-use types are concentrated in the central part of Huacheng Town.

The map of the integrated risk of benggang in Huacheng Town is obtained by overlaying the erosion risk with the disaster risk of three land-use types. Utilizing a natural breakpoint method, this risk is categorized into high, medium, and low levels (Figure 9d). The respective area proportions are 12.17%, 62.05%, and 25.78%. This visualization offers a comprehensive understanding of the areas in Huacheng Town most susceptible to benggang hazards. It facilitates targeted planning for risk-mitigation and management measures, providing a strategic basis for effective interventions.

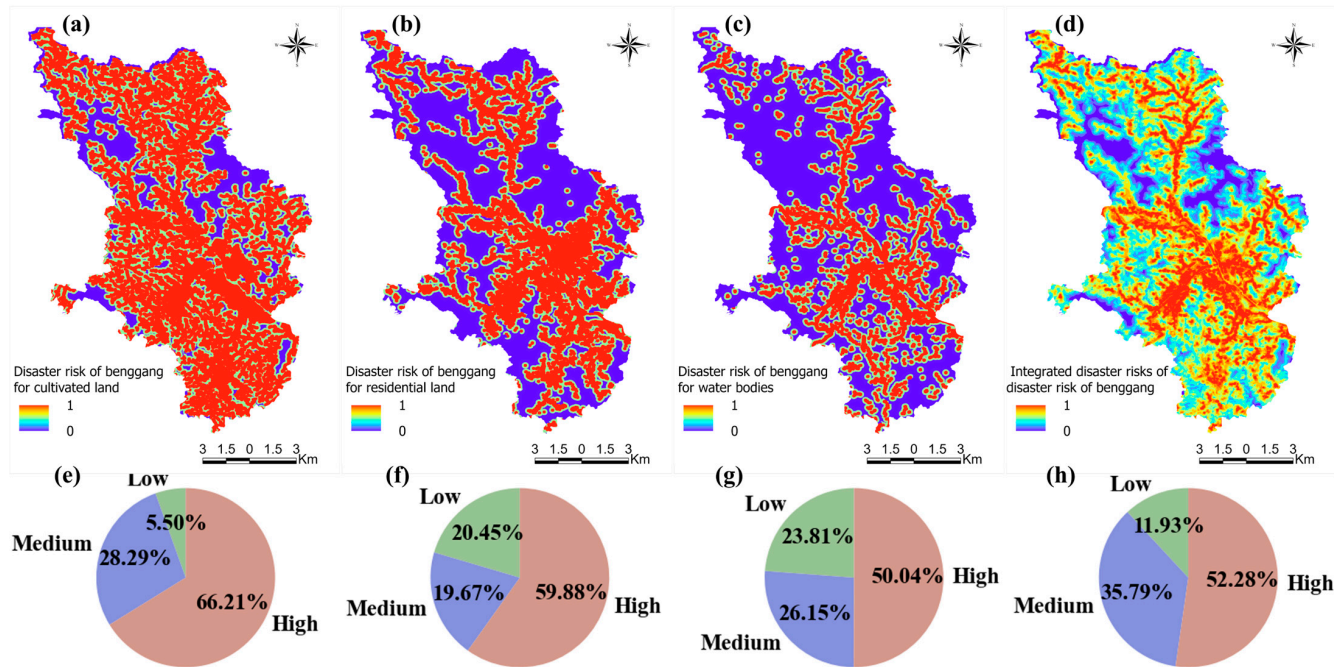


Figure 8. Disaster risk of benggang for cultivated land, residential land, and water bodies in Huacheng Town. (a) is the spatial distribution of the disaster risk of benggang for cultivated land, and (e) is the proportion of high, medium, and low disaster risk for cultivated land; (b,f) is the disaster risk of benggang for residential land; (c,g) is the disaster risk of benggang for water bodies; and (d,h) is integrated disaster risk of benggang.

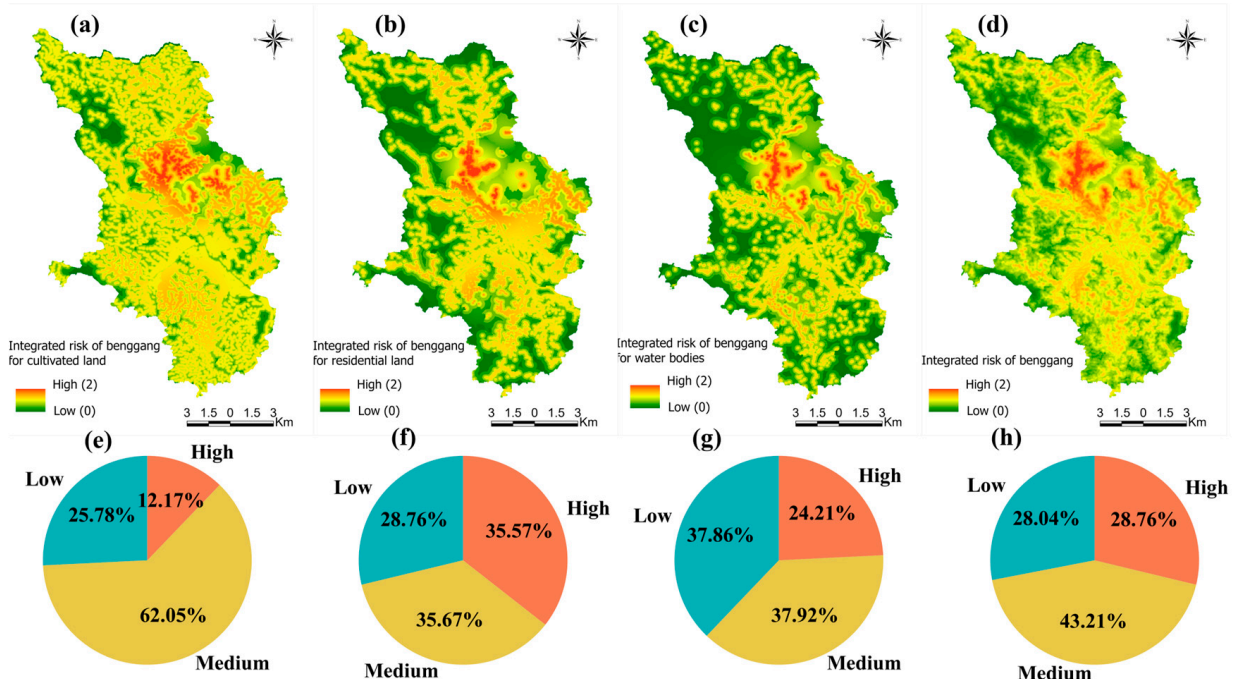


Figure 9. Integrated risk of benggang for cultivated land, residential land, and water bodies in Huacheng Town. (a) is the spatial distribution of the integrated risk of benggang for cultivated land, and (e) is the proportion of high, medium, and low integrated risk for cultivated land; (b,f) is the integrated risk of benggang for residential land; (c,g) is the integrated risk of benggang for water bodies; and (d,h) is integrated risk of benggang.

3.4. The Priority of Benggang Management

Effectively addressing the numerous benggang in Huacheng Town requires a systematic analysis of the priority for benggang management. By combining the distribution of benggang (Figure 4a) with the integrated benggang risk (Figure 9) using the “extract value to point” function in ArcGIS, a sorted list of benggang was generated and was categorized into three priority levels: high, medium, and low. Sorting was done in descending order, with a higher integrated-risk value indicating a greater hazard and higher management priority.

Benggang, with high priority for management, demonstrates both high benggang risk and high disaster risk. Concentrating resources on these areas enhances resource utilization efficiency and is expected to yield significant management effects. Even benggang with medium or low management priority, while having relatively lower urgency, should be selected for management to understand the development process, enhance management strategies for early and middle stages, and prevent further development.

The amount with the high, medium, and low priority of benggang risk accounted for 20.89%, 45.92%, and 33.19%, areas with proportions of 29.33%, 40.90%, and 29.77%, respectively (Figures 10d and 11). Benggang with high governance priority are mainly concentrated in the central region, accounting for approximately 20%. Those with medium governance priority exceed 40% in each case (Figure 10d). Benggang with low governance priority is mainly distributed in areas far from the town and can be addressed with measures such as vegetation cover.

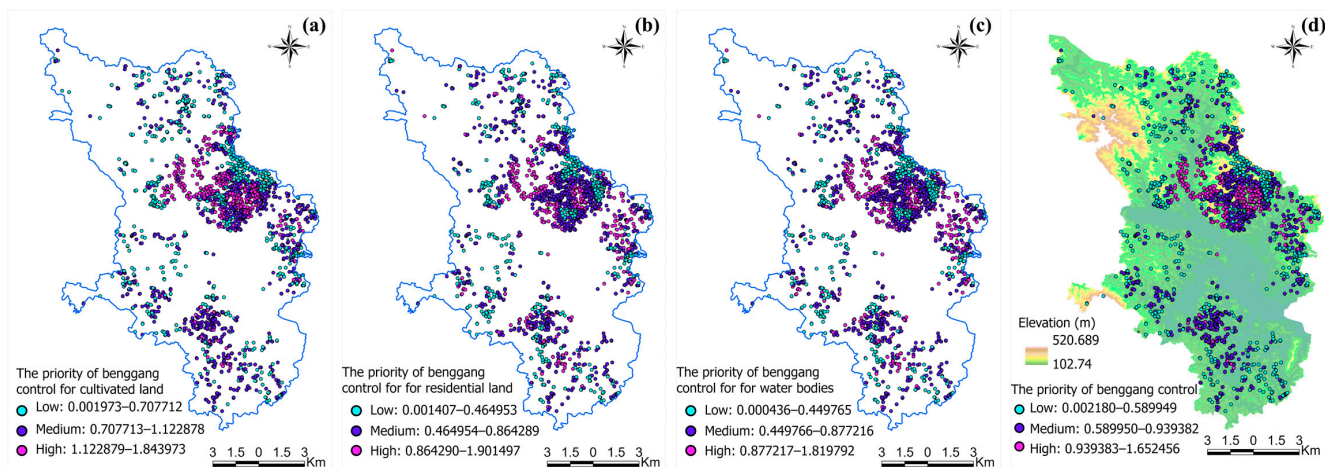


Figure 10. Differentiated priority benggang for various vulnerable entities. (a) is the spatial distribution of the priority of benggang control for cultivated land, (b) is the priority of benggang control for residential land, (c) is the priority of benggang control for water bodies, and (d) is the priority of benggang control.

In addition, the priority of benggang governance is not uniform across different vulnerable entities (Figures 10 and 11). To address this variability, the distribution of benggang and the maps of hazard risk for each vulnerable entity were considered. This led to the derivation of separate governance priorities for cultivated land, residential land, and water bodies.

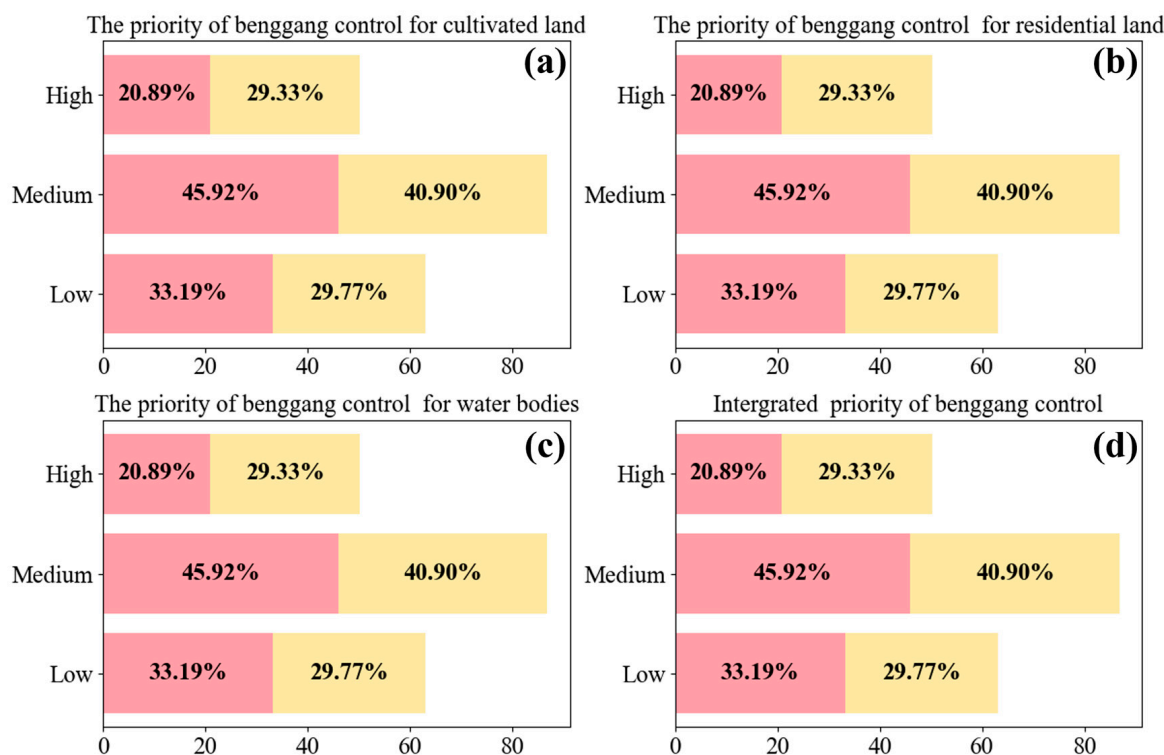


Figure 11. Percentage of count and area of differentiated priority benggang for various vulnerable entities. (a) is the percentage of count and area of the priority of benggang control for cultivated land, (b) is the priority of benggang control for residential land, (c) is the priority of benggang control for water bodies, and (d) is the priority of benggang control.

4. Discussion

4.1. The Identification Method of Benggang

Benggang can be considered to be a special type of eroded landform developed by the separation, collapse, and deposit of hillside soil (rock) on deeply weathered crusts in the tropical and subtropical areas of southern China under the combined action of water and gravity, consisting of an upper catchment area, collapsing walls, colluvial deposit, a main scoured channel, and an alluvial fan, which can be effectively distinguished from similar eroded landforms [15], such as the Lavaka landforms in Madagascar [37], the Calanchi (badland) landforms in Italy [38], and the Voçoroca landforms in Brazil [39]. The benggang of China and Lavaka in Madagascar belongs to the same physiognomy; Brosens, et al. [40] used aerial pictures and satellite imagery to explore the development processes of Lavaka.

The identification of benggang is a crucial aspect of large-scale investigations, erosion management, and understanding erosion mechanisms. Traditional methods relying on field investigations suffer from low automation, high manpower costs, and resource-intensive processes, making them inadequate for large-scale endeavors. For instance, the Yangtze River Water Resources Commission's survey on benggang in southern China took 16 months to complete, highlighting the inefficiency of traditional approaches [12]. The advent of automatic recognition using high-resolution satellite remote-sensing images or UAV images presents new opportunities for efficient and cost-effective identification. Cheng et al. [41] demonstrated automatic landslide detection using a scene-classification method based on the bag-of-visual-words (BoVW) representation. The technology of UAV photography can quickly obtain 360° and multi-angle-image information of benggang for accurately identifying benggang [15]. Recognizing the similarities between landslides and benggang, Shen et al. [28] combined the BoVW model, high-resolution Digital Orthophoto Map, and Digital Surface Model features for benggang representation. Although the recall rate and accuracy rate of Shen et al. [28] have been more than 80%, there are still some

misjudgments. In the future, advanced new technologies such as UAV aerial photography and the extraction of InSAR information should be applied to further improve the efficiency of benggang investigations [15].

In recent times, deep learning algorithms, particularly Transformer architectures, have emerged as promising tools for image feature extraction. Vision transformers like Segformer, Segmenter, UperNet-Swin transformer, and dense prediction transformer have been evaluated, with Segformer demonstrating superior segmentation results on UAV-based and multiscale testing datasets [42,43]. Lin et al. [35] utilized the Segformer model with Sentinel-2 data for wetland classification in Yancheng, China, achieving high accuracy. In our study, the Segformer model demonstrated recognition accuracy exceeding 90% (Table 2). Notably, the Segformer model has shown success in complex tasks, such as weed detection, achieving final mAcc and mIoU of 75.18% and 65.74% [44].

Future research could explore the integration of deep learning models, particularly leveraging drone imagery, to enhance the identification of benggang. This approach holds the potential to generate datasets containing accurate information on the number and location of benggang in southern China. The transition from traditional methods to advanced deep learning techniques represents a significant step forward in automating and improving the efficiency of benggang identification processes.

4.2. Risk-Assessment Method of Benggang and Its Applicability

Soil-erosion risk and prognosis maps play a crucial role in political planning for soil conservation [45]. Nigel and Rughooputh [46] proposed prioritizing soil and water conservation efforts based on the percentage of high erosion areas in basins. Current potential benggang risk-assessment methods involve selecting risk factors such as river network buffer distance, slope, elevation, soil type, vegetation coverage, and land-use type. Models like Information Entropy models, Logistic models, or Sensitivity analysis are then employed to obtain benggang occurrence risk [47]. Cheng et al. [47] utilized an expert scoring method to assign hazard weights for benggang on different land use types and calculated benggang hazard risk. While these methods provide spatial distribution maps for benggang risk, they primarily focus on decision support for potential benggang prevention planning.

However, existing approaches lack clear guidance on the precise management of identified benggang. In our study, we evaluated the integrated risk (Figure 9) by considering benggang erosion risk and disaster risk (Figures 7 and 8). Each benggang was ranked based on its integrated risk, and a priority sequence for benggang management was established (Figure 10). Decision makers can then implement measures such as centralized management, phased management, and enclosure protection, guided by the emphasis on management, comprehensive benggang risk, and spatial distribution.

Defining high-erosion areas poses several possibilities, and validation helps determine the best-correlated classes with high-erosion areas (Figures 9 and 12) [46]. A common challenge in soil-erosion risk mapping is the difficulty of validation, especially with ground truthing [48]. Our study tackled this challenge by combining field surveys and UAVs to verify the accuracy of benggang occurrence risk against actual benggang. UAVs provided enhanced accessibility to benggang sites with challenging terrain. The methodology adopted, encompassing the utilization of UAVs, panoramic photography, and prompt ground truth verification, significantly improves the precision and efficiency of benggang risk evaluation (<https://www.720yun.com/>, accessed on 19 August 2022). We show the panorama of the benggang in Figure 3c (<https://www.720yun.com/vr/1c3jkdeata2>, accessed on 19 August 2022). The adaptable nature of this mapping approach makes it transferable to other regions and countries requiring erosion assessments for the identification of high-erosion areas and priority action areas.

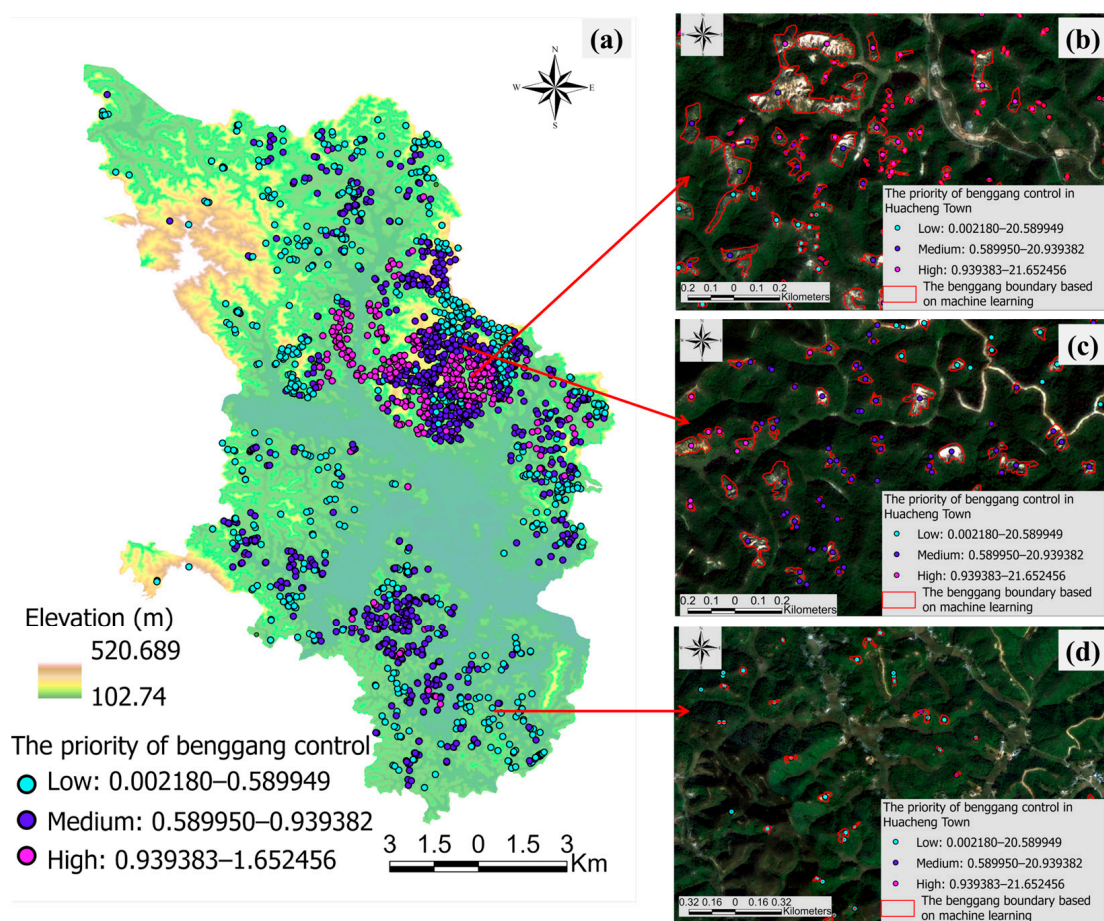


Figure 12. Differentiated priority benggang. (a) is the spatial distribution of the priority of benggang control, and (c–d) show the features of high, medium, and low priority in high-resolution images (GF-1), respectively.

4.3. Implications on Policy Making and Nature-Based Solutions

The interactions among climate, ecosystems, and human society underpin emerging risks, emphasizing the need for effective risk assessments. Nature-based solutions (NbS) are recognized as fundamental approaches to addressing natural hazards and climate risks, defined as actions that protect [49], sustainably manage, and restore natural or modified ecosystems, simultaneously providing benefits to human well-being and biodiversity [50]. Smith et al. [51] highlight the effectiveness of NbS, particularly against landslides and erosion events, through interventions that reinforce slopes with vegetation. NbS can systematically analyze and manage the causes of disasters, contributing to the reduction of social and economic vulnerability [52]. This study, by providing benggang management priorities, aligns with the NbS approach, emphasizing the significance of considering cost and benefits comprehensively when formulating treatment plans (Figure 13). Wang et al. (2022) discussed the influence of the roots of *Dicranopteris dichotoma* on the unconfined compressive strength and shear strength of soil on collapsing walls (Figure 13a).

Managing all benggang simultaneously is an ambitious goal. Therefore, the study focuses on providing relevant departments with high-priority benggang areas for management. The idea of system restoration and comprehensive treatment is crucial, where treatment plans should be formulated hierarchically, considering both engineering measures and NbS. The spatial-aggregation characteristics of benggang occurrence, as highlighted in Section 3.2, suggest that high-intensity treatment and restoration should be concentrated in areas with dense spatial distribution and high management priority. The study proposes a management plan based on engineering measures for areas with high management priority,

while low-priority areas can be protected through enclosure or establishing protected zones. Certainly, this study assumes that the larger the benggang area, the greater the erosion risk in its assessment of benggang erosion risk. However, beyond the area of benggang, the developmental stage of the benggang is also a critical factor to consider, typically divided into active, semi-stable, and stable stages. If a benggang is in an active phase, increased management intensity is required even if its risk level is classified as low. Conversely, if the benggang is in a stable phase, efforts should be focused on preventing the reactivation of the benggang. In low-risk areas, active involvement of the local population is encouraged to enhance initiative and community engagement in prevention and protection measures. This aligns with the concept of mobilizing local communities, promoting awareness, and fostering a sense of responsibility for soil erosion prevention.



Figure 13. Management strategies of priority benggang based on nature-based solutions. (a) is a biological measure of benggang control based on the natural restoration of *Dicranopteris dichotoma*, (b) is a biological measure based on *Miscanthus* of benggang/flood fan, and (c) is a biological measure for the control of benggang based on bamboo.

The work emphasizes the role of risk maps not only in identifying and prioritizing high-risk areas but also in raising awareness among farmers and authorities. For benggang with low priority, the study suggests mobilizing community initiatives for future prevention and protection measures according to the development stage [31]. This information can be made accessible digitally, serving as a tool to simplify and standardize enforcement in soil erosion prevention, showcasing successful cooperation between science, policy, and practice [45].

5. Conclusions

The utilization of the Segformer model in this study demonstrated remarkable precision in the identification of benggang, as evidenced by IoU and Acc metrics reaching 93.17 and 96.73, respectively. Spatial distribution analysis unveiled a heightened density of benggang in the central area, with small benggang constituting a substantial portion at 62.4%. The proportional distribution of areas for small, medium, and large benggang were 10.14%, 24.76%, and 65.10%, respectively. Examining high-risk areas, including cultivated land, residential land, and water bodies, revealed a concentration in the central region of Huacheng Town, collectively constituting over 50% of the total. Prioritization for benggang management was classified into high, medium, and low categories, with count proportions of 20.89%, 45.92%, and 33.19%, and area proportions of 29.33%, 40.90%, and 29.77%, respectively. Concentrating resources on areas designated as high priority for management enhances the efficiency of resource utilization and is anticipated to yield significant management effects. Even benggang assigned medium or low management priority, while presenting relatively lower urgency, should be considered for management interventions to comprehend their developmental processes. This approach facilitates the enhancement of management strategies based on nature-based solutions, particularly during the early and middle stages, aiming to prevent further development. The strategic allocation of resources based on this prioritization provides an effective framework for addressing benggang with varying levels of risk, thereby contributing to the formulation and implementation of efficient management strategies for the region.

Author Contributions: X.Y.: Conceptualization, Data curation, Investigation, Methodology, Software, Supervision, Visualization, Writing—original draft, Writing—review & editing. S.G.: Data curation, Formal analysis, Investigation, Methodology. H.J.: Data curation, Methodology. Z.S.: Data curation, Investigation. N.W.: Writing—review & editing. S.Z.: Software, Visualization. L.Y.: Writing—review & editing. M.W.: Data curation, Investigation, Methodology. All authors have read and agreed to the published version of the manuscript.

Funding: This work was supported by the GDAS' Project of Science and Technology Development [2022GDASZH-2022010105; 2023GDASZH-2023010103], the National Natural Science Foundation of China [41301301], and Anhui Provincial Natural Science Foundation [22085US21].

Data Availability Statement: The data presented in this study are available on request from the corresponding author.

Acknowledgments: We would also like to thank Jun Song of the Guangzhou Institute of Geography for his help in the data analysis and Jinbo Xie of the Wuhua Water Conservation Station for his support in the field verification.

Conflicts of Interest: The authors declare that they have no known competing financial interests or personal relationships that could have appeared to influence the work reported in this paper.

References

1. Amundson, R.; Berhe, A.A.; Hopmans, J.W.; Olson, C.; Sztein, A.E.; Sparks, D.L. Soil science. Soil and human security in the 21st century. *Science* **2015**, *348*, 1261071. [[CrossRef](#)] [[PubMed](#)]
2. Borrelli, P.; Alewell, C.; Alvarez, P.; Anache, J.A.A.; Baartman, J.; Ballabio, C.; Bezak, N.; Biddoccu, M.; Cerdà, A.; Chalise, D.; et al. Soil erosion modelling: A global review and statistical analysis. *Sci. Total Environ.* **2021**, *780*, 146494. [[CrossRef](#)] [[PubMed](#)]
3. Xu, L.; Xu, X.; Meng, X. Risk assessment of soil erosion in different rainfall scenarios by RUSLE model coupled with Information Diffusion Model: A case study of Bohai Rim, China. *CATENA* **2012**, *100*, 74–82. [[CrossRef](#)]
4. Zhang, H.; Zhang, J.; Zhang, S.; Yu, C.; Sun, R.; Wang, D.; Zhu, C.; Zhang, J. Identification of Priority Areas for Soil and Water Conservation Planning Based on Multi-Criteria Decision Analysis Using Choquet Integral. *Int. J. Environ. Res. Public Health* **2020**, *17*, 1331. [[CrossRef](#)] [[PubMed](#)]
5. Schmaltz, E.M.; Johannsen, L.L.; Thorsøe, M.H.; Tähtikarhu, M.; Räsänen, T.A.; Darboux, F.; Strauss, P. Connectivity Elements and Mitigation Measures in Policy-Relevant Soil Erosion Models: A Survey across Europe. *Catena* **2024**, *234*, 107600. [[CrossRef](#)]
6. Hu, Y.; Tian, G.; Mayer, A.L.; He, R. Risk assessment of soil erosion by application of remote sensing and GIS in Yanshan Reservoir catchment, China. *Nat. Hazards* **2015**, *79*, 277–289. [[CrossRef](#)]
7. Bamutaze, Y.; Mukwaya, P.; Oyama, S.; Nadhom, D.; Nsemire, P. Intersecting RUSLE modelled and farmers perceived soil erosion risk in the conservation domain on mountain Elgon in Uganda. *Appl. Geogr.* **2020**, *126*, 102366. [[CrossRef](#)]
8. Xu, J. Benggang Erosion: The Influencing Factors. *Catena* **1996**, *27*, 249–263.
9. Wei, Y.; Liu, Z.; Wu, X.; Zhang, Y.; Cui, T.; Cai, C.; Guo, Z.; Wang, J.; Cheng, D. Can Benggang Be Regarded as Gully Erosion? *Catena* **2021**, *207*, 105648. [[CrossRef](#)]
10. Sun, K.; Cheng, D.B.; He, J.J.; Zhao, Y.L. Comparison of two occurrence risk assessment methods for collapse gully erosion—A case study in Guangdong province. *IOP Conf. Series Earth Environ. Sci.* **2018**, *113*, 012209. [[CrossRef](#)]
11. Liu, X. Benggang Erosion Landform and Research Progress in a Global Perspective. *Prog. Geogr.* **2018**, *37*, 342–351.
12. Feng, M. Investigation on Status of Hill Collapsing and Soil Erosion in Southern China. *Yangtze River* **2009**, *40*, 66–68.
13. Deng, Y.; Shen, X.; Xia, D.; Cai, C.; Ding, S.; Wang, T. Soil Erodibility and Physicochemical Properties of Collapsing Gully Alluvial Fans in Southern China. *Pedosphere* **2019**, *29*, 102–113. [[CrossRef](#)]
14. Wang, X.; Cai, Q. Systematic Analysis on Dilapidated Granite and Measures for Management. *Soil Water Conserv. China* **2007**, *7*, 29–3160.
15. Zhu, X.; Gao, L.; Wei, X.; Li, T.; Shao, M. Progress and prospect of studies of Benggang erosion in southern China. *Geoderma* **2023**, *438*, 116656. [[CrossRef](#)]
16. Zhang, D.; Liu, X. Evolution and Phases Division of Collapsed Gully Erosion Landform. *J. Subtrop. Resour. Environ.* **2011**, *6*, 23–28.
17. Duan, X.; Deng, Y.; Tao, Y.; He, Y.; Lin, L.; Chen, J. The soil configuration on granite residuals affects Benggang erosion by altering the soil water regime on the slope. *Int. Soil Water Conserv. Res.* **2021**, *9*, 419–432. [[CrossRef](#)]
18. Jiang, F.; He, K.; Huang, M.; Zhang, L.; Lin, G.; Zhan, Z.; Li, H.; Lin, J.; Ge, H.; Huang, Y. Impacts of near soil surface factors on soil detachment process in benggang alluvial fans. *J. Hydrol.* **2020**, *590*, 125274. [[CrossRef](#)]
19. Liao, Y.; Tang, C.; Yuan, Z.; Zhuo, M.; Huang, B.; Nie, X.; Xie, Z.; Li, D. Research Progress on Benggang Erosion and Its Prevention Measure in Red Soil Region of Southern China. *Acta Pedol. Sin.* **2018**, *55*, 1297–1312.
20. Ji, X.; Huang, Y.; Lin, J.; Jiang, F.; Hongli, G.E. Spatio-Temporal Erosion Features and Prediction for the Erosion Gullies on Collapsing Hills. *Mt. Res.* **2019**, *37*, 86–97. [[CrossRef](#)]
21. Cai, L.; Liu, M.X.; Hou, X.L.; Wu, P.F.; Ma, X.Q. Comparison of Plant Diversity among Different Governance Models in Collapsing Gully Erosion Area of Changting County. *J. Fujian Agric. For. Univ. (Nat. Sci. Ed.)* **2012**, *41*, 524–528.

22. Xia, J.; Cai, C.; Wei, Y.; Wu, X. Granite residual soil properties in collapsing gullies of south China: Spatial variations and effects on collapsing gully erosion. *CATENA* **2019**, *174*, 469–477. [[CrossRef](#)]
23. Wu, C. Landslide Susceptibility Based on Extreme Rainfall-Induced Landslide Inventories and the Following Landslide Evolution. *Water* **2019**, *11*, 2609. [[CrossRef](#)]
24. Wei, Y.; Wu, X.; Wang, J.; Yu, H.; Xia, J.; Deng, Y.; Zhang, Y.; Xiang, Y.; Cai, C.; Guo, Z. Identification of geo-environmental factors on Benggang susceptibility and its spatial modelling using comparative data-driven methods. *Soil Tillage Res.* **2021**, *208*, 104857. [[CrossRef](#)]
25. Damm, B.; Klose, M. The landslide database for Germany: Closing the gap at national level. *Geomorphology* **2015**, *249*, 82–93. [[CrossRef](#)]
26. Sharir, K.; Roslee, R.; Lee, K.E.; Simon, N. Landslide Factors and Susceptibility Mapping on Natural and Artificial Slopes in Kundasang, Sabah. *Sains Malays.* **2017**, *46*, 1531–1540. [[CrossRef](#)]
27. Liao, Y.; Zheng, M.; Li, D.; Wu, X.; Liang, C.; Nie, X.; Huang, B.; Xie, Z.; Yuan, Z.; Tang, C. Relationship of benggang number, area, and hypsometric integral values at different landform developmental stages. *Land Degrad. Dev.* **2020**, *31*, 2319–2328. [[CrossRef](#)]
28. Shen, S.; Zhang, T.; Cheng, D.; Wang, Z.; Zhao, Y.; Deng, Y.; Qian, F. Benggang Recognition on Semantic Fusion of High-Resolution Digital Orthophoto Map and Digital Surface Model Data from Unmanned Aerial Vehicle. *Trans. Chin. Soc. Agric. Eng.* **2020**, *36*, 69–79.
29. Zhou, X.; Yu, H.; Wei, Y.; Hu, J.; Cai, C. Method for Monitoring Change in Benggang Erosion Based on Oblique Aerial Images of Uav. *Trans. Chin. Soc. Agric. Eng.* **2019**, *35*, 51–59.
30. Liu, H.; Liu, X.; Zhang, P.; Wang, Y. Characteristics of Slope Collapse and Its Monitoring Technology in Southern China. *Sci. Soil Water Conserv.* **2011**, *9*, 19–23.
31. Liao, Y.; Yuan, Z.; Li, D.; Zheng, M.; Huang, B.; Xie, Z.; Wu, X.; Luo, X. What Kind of Gully Can Develop into Benggang? *Catena* **2023**, *225*, 107024. [[CrossRef](#)]
32. Liu, X.; Qiu, J.; Zhang, D. Characteristics of slope runoff and soil water content in benggang colluvium under simulated rainfall. *J. Soils Sediments* **2018**, *18*, 39–48. [[CrossRef](#)]
33. Liu, X.; Zhang, D. Grain-size properties and morphologic patterns of channelized flows in a benggang catchment of southern China. *Zeitschrift für Geomorphologie* **2018**, *61*, 303–314. [[CrossRef](#)]
34. Chen, C.; Jiang, H.; Liu, X.; Huang, G.; Lai, Y.; Jing, W. Spatial Differentiation of Pond Landscapes across an Urban-Rural Gradient in the Pearl River Delta Region. *Water* **2022**, *14*, 1637. [[CrossRef](#)]
35. Lin, X.; Cheng, Y.; Chen, G.; Chen, W.; Chen, R.; Gao, D.; Zhang, Y.; Wu, Y. Semantic Segmentation of China's Coastal Wetlands Based on Sentinel-2 and Segformer. *Remote Sens.* **2023**, *15*, 3714. [[CrossRef](#)]
36. Li, T.; Wang, C.; Wu, F.; Zhang, H.; Tian, S.; Fu, Q.; Xu, L. Built-Up Area Extraction from GF-3 SAR Data Based on a Dual-Attention Transformer Model. *Remote Sens.* **2022**, *14*, 4182. [[CrossRef](#)]
37. Wells, N.A.; Andriamihaja, B.; Rakotovololona, H.F.S. Patterns of Development of Lavaka, Madagascar Unusual Gullies. *Earth Surf. Process. Landf.* **1991**, *16*, 189–206. [[CrossRef](#)]
38. Neugirg, F.; Stark, M.; Kaiser, A.; Vlachilova, M.; Della Seta, M.; Vergari, F.; Schmidt, J.; Becht, M.; Haas, F. Erosion processes in calanchi in the Upper Orcia Valley, Southern Tuscany, Italy based on multitemporal high-resolution terrestrial LiDAR and UAV surveys. *Geomorphology* **2016**, *269*, 8–22. [[CrossRef](#)]
39. Bacellar, L.D.P.; Netto, A.L.C.; Lacerda, W.A. Controlling Factors of Gullying in the Maracuja Catchment, Southeastern Brazil. *Earth Surf. Process. Landf.* **2005**, *30*, 1369–1385. [[CrossRef](#)]
40. Brosens, L.; Broothaerts, N.; Campforts, B.; Jacobs, L.; Razanamahandry, V.F.; Van Moerbeke, Q.; Bouillon, S.; Razafimbelo, T.; Rafolisy, T.; Govers, G. Under pressure: Rapid lavaka erosion and floodplain sedimentation in central Madagascar. *Sci. Total. Environ.* **2022**, *806*, 150483. [[CrossRef](#)]
41. Cheng, G.; Guo, L.; Zhao, T.; Han, J.; Li, H.; Fang, J. Automatic landslide detection from remote-sensing imagery using a scene classification method based on BoVW and pLSA. *Int. J. Remote Sens.* **2012**, *34*, 45–59. [[CrossRef](#)]
42. Li, M.; Rui, J.; Yang, S.; Liu, Z.; Ren, L.; Ma, L.; Li, Q.; Su, X.; Zuo, X. Method of Building Detection in Optical Remote Sensing Images Based on SegFormer. *Sensors* **2023**, *23*, 1258. [[CrossRef](#)]
43. Gonçalves, D.N.; Marcato, J.; Carrilho, A.C.; Acosta, P.R.; Ramos, A.P.M.; Gomes, F.D.G.; Osco, L.P.; Oliveira, M.d.R.; Martins, J.A.C.; Damasceno, G.A.; et al. Transformers for mapping burned areas in Brazilian Pantanal and Amazon with PlanetScope imagery. *Int. J. Appl. Earth Obs. Geoinf.* **2023**, *116*, 103151. [[CrossRef](#)]
44. Jiang, K.; Afzaal, U.; Lee, J. Transformer-Based Weed Segmentation for Grass Management. *Sensors* **2022**, *23*, 65. [[CrossRef](#)]
45. Prasuhn, V.; Liniger, H.; Gisler, S.; Herweg, K.; Candinas, A.; Clément, J.-P. A high-resolution soil erosion risk map of Switzerland as strategic policy support system. *Land Use Policy* **2013**, *32*, 281–291. [[CrossRef](#)]
46. Nigel, R.; Rughooputh, S. Mapping of monthly soil erosion risk of mainland Mauritius and its aggregation with delineated basins. *Geomorphology* **2010**, *114*, 101–114. [[CrossRef](#)]
47. Cheng, D.; Zhao, Y.; Zhang, P.; Zhao, J. On the Risk Assessment of Collapse Gully Erosion in Jiangxi Province Based on Logistic Model. *Sci. Soil Water Conserv.* **2017**, *36*, 27.
48. Van Rompaey, A.J.J.; Govers, G. Data Quality and Model Complexity for Regional Scale Soil Erosion Prediction. *Int. J. Geogr. Inf. Sci.* **2002**, *16*, 663–680. [[CrossRef](#)]

49. Reguero, B.G.; Renaud, F.G.; Van Zanten, B.; Cohen-Shacham, E.; Beck, M.W.; Di Sabatino, S.; Jongman, B. Editorial: Nature-based solutions for natural hazards and climate change. *Front. Environ. Sci.* **2022**, *10*, 1101919. [[CrossRef](#)]
50. Seddon, N.; Smith, A.; Smith, P.; Key, I.; Chausson, A.; Girardin, C.; House, J.; Srivastava, S.; Turner, B. Getting the message right on nature-based solutions to climate change. *Glob. Chang. Biol.* **2021**, *27*, 1518–1546. [[CrossRef](#)]
51. Smith, A.C.; Tasnim, T.; Irfanullah, H.M.; Turner, B.; Chausson, A.; Seddon, N. Nature-based Solutions in Bangladesh: Evidence of Effectiveness for Addressing Climate Change and Other Sustainable Development Goals. *Front. Environ. Sci.* **2021**, *9*, 737659. [[CrossRef](#)]
52. Marušić, B.G.; Dremel, M.; Ravnikar, Ž. A Frame of Understanding to Better Link Nature-Based Solutions and Urban Planning. *Environ. Sci. Policy* **2023**, *146*, 47–56. [[CrossRef](#)]

Disclaimer/Publisher's Note: The statements, opinions and data contained in all publications are solely those of the individual author(s) and contributor(s) and not of MDPI and/or the editor(s). MDPI and/or the editor(s) disclaim responsibility for any injury to people or property resulting from any ideas, methods, instructions or products referred to in the content.